Chapter 2

IMPOL–Design and Construction

In the last chapter, we had traced the growth of polarimetry to the status of a powerful observational aid of the modern day astronomer. We also saw the advantages of imaging polarimetric techniques over single aperture polarimetry. In this chapter we discuss the key issues which are associated with the design and construction of an imaging polarimeter. In the first section, we lay down a set of goals and guidelines, which have been adopted as the basis for the construction of the instrument. The basic optical principle employed for polarimetry in this instrument is presented in section 2.2, which is followed by a description of the various pre-fabrication laboratory tests carried on the various components, in section 2.3. The three sections which follow deal with the details relevant to the fabrication of the instrument.

2.1 Scientific Goals and Technical Guidelines

In order to undertake observations, such as that are discussed in Sec. 1.2.2, we need an instrument with a field of view of a few arcminutes, an optics well matched with the telescope to minimize loss of light and a detector of sufficient sensitivity. Also, we need to eliminate the effects of atmospheric scintillation and minimize instrumental polarization and other sources of uncertainties so that polarization could be measured with accuracies better than 0.1% .

It is required to ensure that the images on the CCD surface do not move during observations. For this, we need to choose a design which has the minimum number of moving components in the optical path. We also need to keep the tracking errors less than the width of the point spread function. The mechanical design should be such that flexures at different telescope orientations also do not cause image motion. Since the objects of interest are often faint, the instrument should have an acquisition facility with pointing accuracy of a few arcseconds.

Information about the size distribution of grains responsible for producing dichroic scattering can be obtained by studying the wavelength dependence of polarization.

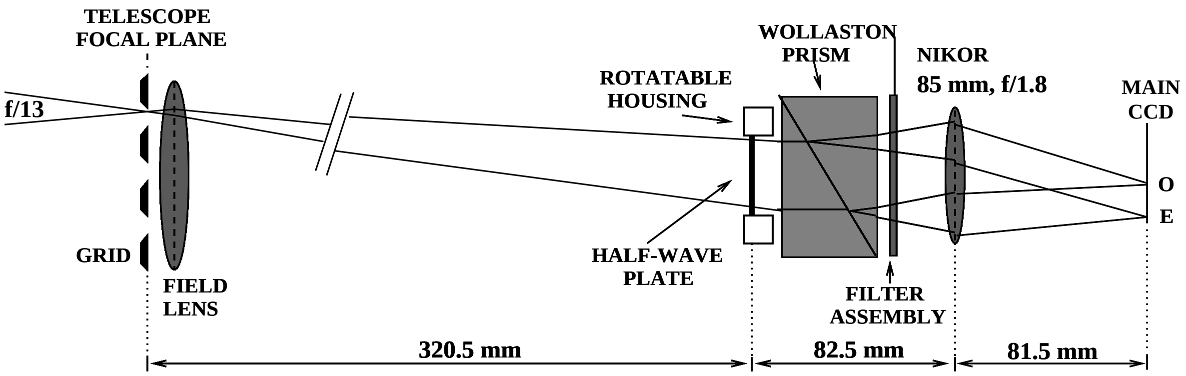

Figure 2.1: Block schematic of the IMPOL optical system

Hence it is emphasized that the instrument should be capable of making multi-wavelength observations in various wavelength bands in the optical and near-IR regions.

To facilitate easy mounting of the instrument on the telescope, the entire assembly consisting of the optics, acquisition and guidance unit, associated electronics etc. is to be designed as a self-contained unit which can be easily mounted on the telescope, with only electrically isolated communication links to the computers for instrument control and data acquisition. The cost of the instrument is to be minimized by using standard optical and electronic components and by avoiding over-specification as far as possible.

The two largest telescope facilities in India, are the 2.3 m, f/13 Vainu Bappu Telescope (VBT) at Kavalur and the 1.2 m, f/13 Gurushikhar Infrared Telescope (GIRT) at Mt. Abu. The design and construction of the instrument is to be in such a way that it can be used at either of these facilities.

2.2 Optical principle of the instrument

The principle of the instrument (Sen & Tandon 1994) is based on a combination of ideas suggested by Ohman (1939) and Appenzeller (1967); an instrument of this type has been constructed at the University of Durham and has been in use for some time now (Scarrott et. al. 1983). A schematic of the optical system of IMPOL is shown in Fig. 2.1.

The instrument has a camera lens (Nikkor 85 mm, f/1.8) which acts as a focal reducer that reimages the telescope focal plane on the surface of a CCD, with a reduction factor of about 3.8. A Wollaston prism is placed in the optical path just before the camera lens. Once light passes through the Wollaston prism it is split into two orthogonal polarization components parallel and perpendicular to the axis of the Wollaston prism. These two components (usually called the ordinary and the extraordinary components – see Sec. C.1) travel in slightly different directions, separated, in this case, by about 0.5°. This results in two images being produced on the CCD for every point at the telescope focal plane. The ratio (R) of the difference between the intensities in the ordinary (I_o) and the extraordinary (I_e) images to their sum is the normalized Stokes parameter q, defined in a coordinate system aligned with the axes of the Wollaston prism (see App. A).

According to the discussion following Eq. A.2, in order to determine the degree of linear polarization p and its position angle θ, it is necessary to measure the above ratio for two orientations of the Wollaston prism, for example 0° and 45°. Equivalently, the same can be accomplished by placing a half-wave plate (HWP) on a rotatable mount preceding the Wollaston prism and keeping the Wollaston prism itself fixed with respect to the instrument axes. The property of the HWP is to add an additional phase shift of 180° to the polarization eigen vector parallel to its fast-axis. Thus effectively when the HWP is rotated through an angle α, the plane of polarization of light passing through it will be rotated through an angle 2α. Therefore by rotating the HWP through 22.5°, and determining the ratio as above, the second Stokes parameter u also may be determined. Thus

$$q = \frac{I_o(0^\circ) - I_e(0^\circ)}{I_o(0^\circ) + I_e(0^\circ)} \qquad \text{and} \qquad u = \frac{I_o(22.5^\circ) - I_e(22.5^\circ)}{I_o(22.5^\circ) + I_e(22.5^\circ)} \; . \tag{2.1}$$

Whenever it is convenient, we will use the notation $R(\alpha)$, to denote the ratios of the form in Eq. 2.1, where α denotes the position angle of the HWP.

To arrive at the relations connecting (p, θ) with (q, u), we need to understand how the unpolarized and polarized parts of the light get modulated as it passes through the HWP followed by the Wollaston prism. As far as the unpolarized part is concerned, it is unaffected by the orientation of the HWP, but is split into two equal halves by the Wollaston prism. But the progress of the polarized part of light is more complicated and is illustrated in Fig. 2.2.

In part (a) of the figure, the axis of the HWP is aligned with that of the Wollaston prism. The polarization vector is shown to make an angle θ with the slow-axis of the HWP. Once it comes out of the HWP it has been rotated through an angle 2θ. At the Wollaston prism the light is split into two polarization components, the amplitudes of the electric fields of which are proportional to $\cos(\theta)$ and $\sin(\theta)$. Hence the intensities in the ordinary and the extra-ordinary images due to the polarized part will be proportional to $\cos^2(\theta)$ and $\sin^2(\theta)$. In part (b) we consider the more general case when the HWP fast-axis is oriented at an angle α to the axis of the Wollaston prism. As illustrated, in this case the two intensities are proportional to $\cos^2(\theta - 2\alpha)$ and $\sin^2(\theta - 2\alpha)$. Therefore the total intensities in the ordinary and extra-ordinary images due to both the polarized and unpolarized components are given by

$$I_o = \frac{I_{up}}{2} + I_p \cos^2(\theta - 2\alpha) \qquad \text{and} \qquad I_e = \frac{I_{up}}{2} + I_p \sin^2(\theta - 2\alpha) \; . \tag{2.2}$$

Now the difference-to-sum ratio of the intensities is given by

$$\frac{I_o(\alpha) - I_e(\alpha)}{I_o(\alpha) + I_e(\alpha)} = \frac{I_p}{I_{up} + I_p} \cos(2\theta - 4\alpha) = p \cos(2\theta - 4\alpha) \; . \tag{2.3}$$

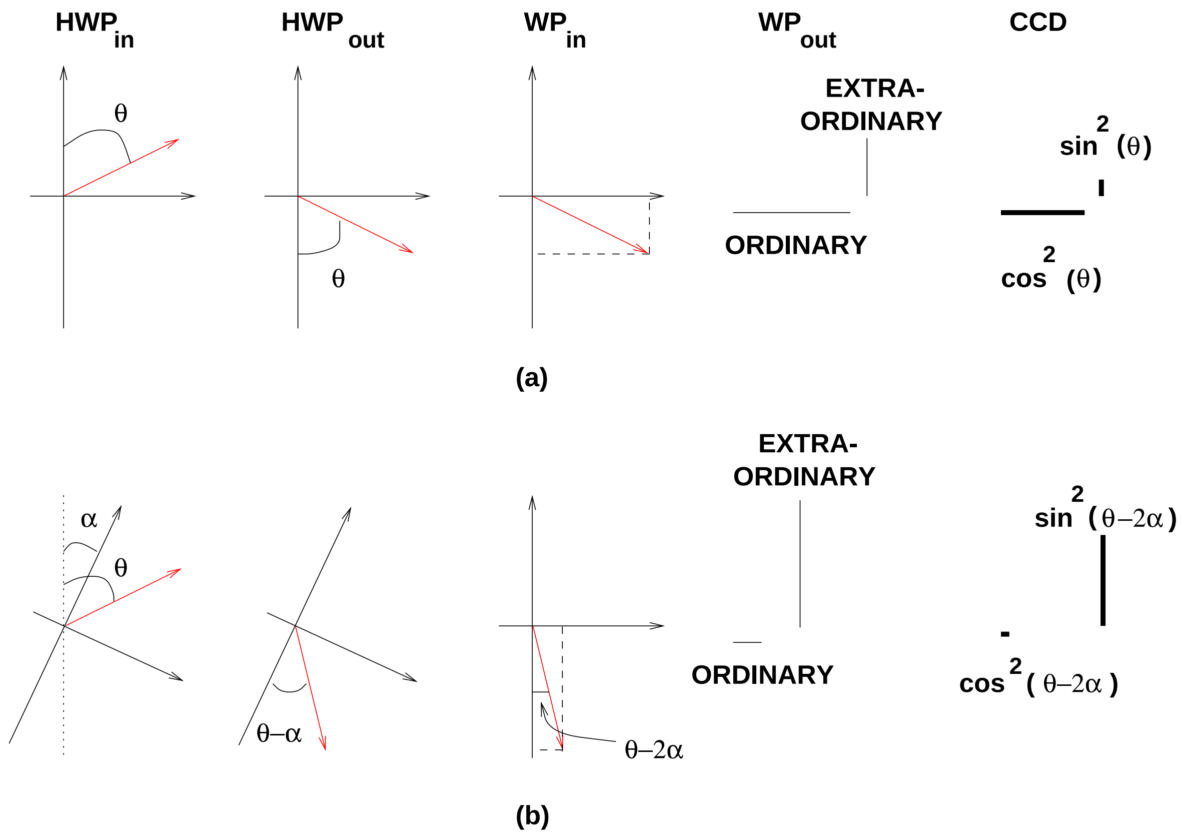

Figure 2.2: Modulation of Polarization of Light in the Imaging Polarimeter

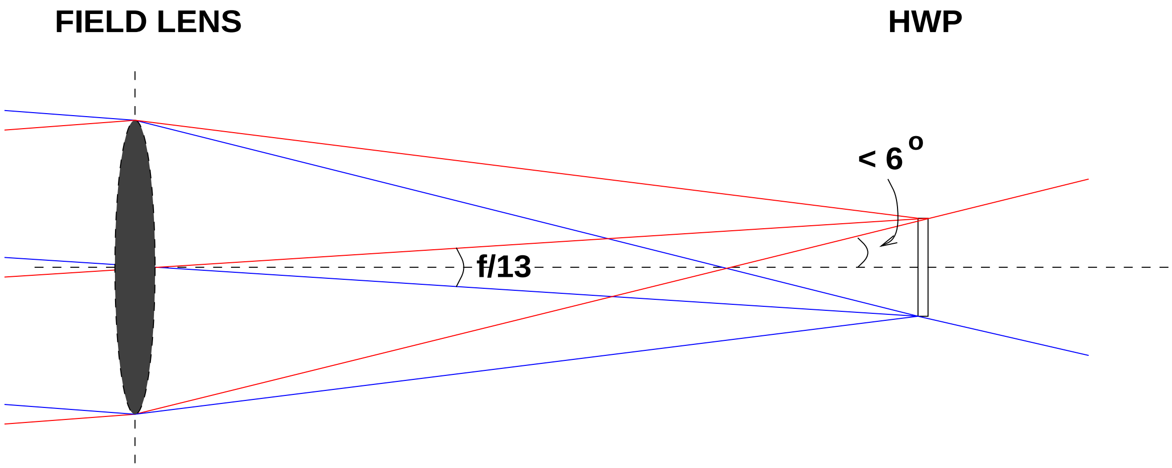

Figure 2.3: Field lens and Half-wave plate in the polarimeter

Thus the basic equation of the instrument which relates the measured quantities (I_o,I_e) to the parameters to be determined (p, θ) is given by

$$\frac{I_o/I_e - 1}{I_o/I_e + 1} = R(\alpha) = p\cos(2\theta - 4\alpha)\ . \tag{2.4}$$

We also find that, on combining this equation with the expressions given in Eq. 2.1 and doing a little algebra, we get the expressions in Eq. A.3.

The HWP is the only moving component in the optical path and hence is the most critical one. It is placed at the focal plane of a field lens, which in turn is placed close to the telescope focal plane. With this arrangement, the entrance pupil (telescope primary) is imaged by the field lens at the position of the HWP and the light beam will have minimum diameter at this position (see Fig. 2.3). Also it can now be ensured that the HWP presents the same part of its surface to the beam from each point of the field of view, irrespective of its rotation.

The optical arrangement described above, produces two images – the ordinary and the extraordinary ones – on the CCD, for every point at the telescope focal plane. In order to avoid overlap of the ordinary and extraordinary images of adjacent points, a set of properly spaced, parallel obscuring strips of the correct width are placed at the telescope focal plane (see Sec. 2.3.4). However, if the targets of observation are point sources, like stars in an uncrowded field, as is often the case, it becomes possible to avoid using the grid, with the advantage of being able to observe the entire field of view. The edges of the obscuring strips are made slanting by more than 5° to avoid vignetting of the f/13 telescope beam at the Cassegrain focii of both the Vainu Bappu telescope and the Gurushikhar telescope.

The only remaining optical component is the filter which is inserted between the Wollaston prism and the camera lens. The filter is put before the camera lens because the beam is slower there, but beyond the analyzer so that any birefringence in it will not affect the measurement of polarization.

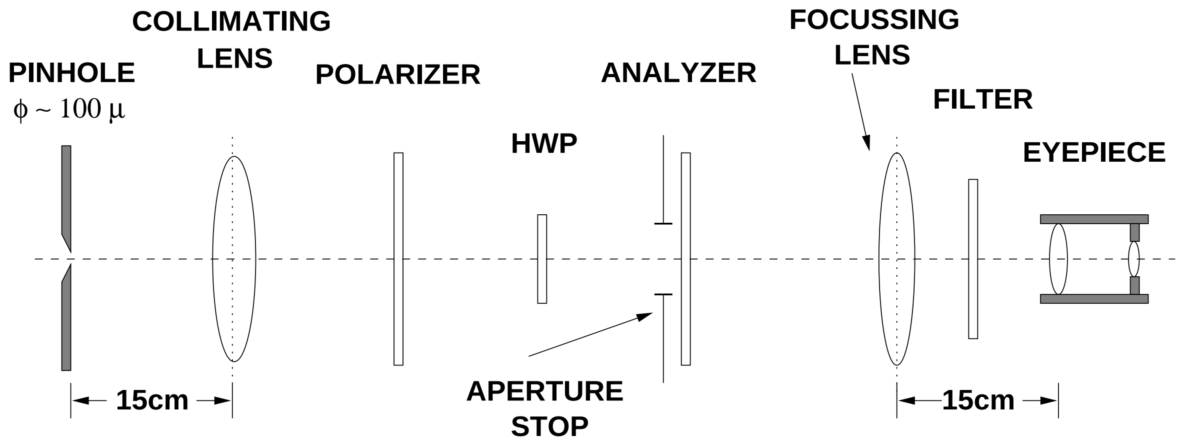

Figure 2.4: Schematic of the optical arrangement for testing the half-wave plate.

Appendix C contains a brief description of some properties of the HWP and the Wollaston prism followed by the Mueller matrix representation of the transfer function of the instrument.

2.3 On the optical bench

Before the optical components described above were assembled in the instrument structure, they were tested individually in the laboratory to verify their performances. Then these components were assembled on the optical bench and their relative positions were adjusted for optimizing the overall performance. In the following sections we briefly describe the methods adopted for these tests and their results.

2.3.1 The half-wave plate (HWP)

The HWP was checked for depolarization produced by dispersion in the retardance and the orientation of the fast axis. It was also tested for non-parallelism of the surfaces, which can lead to image motion, when it is rotated. The optical arrangement used was the same for both the tests and is shown in Fig. 2.4.

Depolarization due to the half-wave plate

Depolarization, in this context, means the conversion of plane polarized light to any other polarization state. The position angle of the fast-axis of the HWP may vary with wavelength even within the operating wavelength band. The retardance also can deviate from π within the bandwidth. These will cause depolarization of light as it passes through the HWP.

The procedure adopted to look for this effect is as follows. Firstly, the polarizer

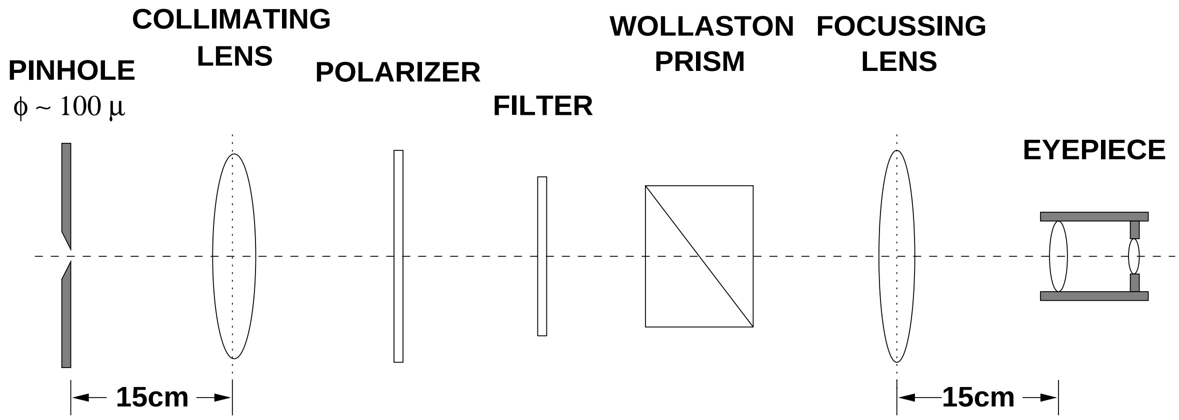

Figure 2.5: Schematic of the optical arrangement for testing the Wollaston prism

and the analyzer are brought to crossed condition without the HWP in between. This is done by rotating the polarizer till the intensity of the pinhole image shows a minimum. This is checked visually at the eyepiece and it is verified that the analyzer positioning is repeatable to better than 0.5°. The eyepiece is replaced by a photometer and a reading is taken at this position. Now the HWP is introduced between the polarizer and the analyzer as shown in Fig. 2.4 and is rotated so that the intensity of the image of the pinhole seen through the eyepiece is again minimum. At this position the HWP fast-axis is either aligned with the axis of the polarizer or is orthogonal to it. Any depolarization caused by the HWP will show up as an increase in the minima obtained with and without the HWP in the beam. Upper limits of depolarization of 0.15% in the V-band and 0.3% in the B-band were obtained. The experiment was not carried out in the R-band because of the excessive near infrared emission from the filament lamp source, contaminating the readings.

Wedge-effect of half-wave plate (HWP) surfaces

The HWP is rotated about the optical axis, while looking for any observable shift in the position of the image in the eyepiece with respect to the cross-hairs. The arrangement has a resolution for detecting deviations as small as 1 arcmin. No such effect was observed.

2.3.2 The Wollaston prism

Chromatism in the separation of the ordinary and extraordinary beams, dependence of the beam separation on the angle of incidence of light, and simultaneity of focusing of the two images were checked in the case of Wollaston prism. Also checked was the shift of the image plane produced by inserting the Wollaston prism in the beam path. The optical arrangement used for these tests is shown in Fig. 2.5. Initially, the polarizer is rotated so that the two images are approximately of the same brightness.

Dispersion in image separation

For the 150 mm focal length focusing lens used, the markings on the eyepiece reticle at 100 μm separation correspond to about 2.3 arcmin. The different filters (B, V and R) are inserted into the beam path one after the other and the image separation in the eyepiece noted. The peak to peak variation in separation for the three bands was found to be less than 1.5 arcmin.

Angle of incidence vs. Separation of beams

Two possible extreme conditions are checked with this experiment. In the first case the Wollaston prism is mounted in such a way that the line joining the ordinary and the extraordinary images is vertical and the collimated beam is incident normally on the Wollaston prism. The midpoint of the two images, separation between them and the image sizes are noted looking through the eyepiece. Now the Wollaston prism is rotated about a vertical axis in one degree steps and the above quantities are noted. The change in beam separation is less than 1.5 arcmin, for $\pm 10°$ angles on either side of normal incidence.

In the second case, the Wollaston prism is mounted so that the line joining the images is horizontal. When it is rotated about a vertical axis as described above, the beam separation changed by about 2.5 arcmin for $\pm 10°$ angle of incidence on either side of normal incidence.

Simultaneous focusing of images

This experiment was carried out to see if the two beams come to focus simultaneously. For this, the eyepiece was moved slightly so that the two images become slightly defocused. The sizes of the images are noted from the reticle scale with an accuracy of 50 μm. In all the three filters, the two beams were found to come into focus at the same plane.

2.3.3 The camera lens

The camera lens was tested to see if there is vignetting of the incident beam for off-axis points in the object plane. The experimental set up for this is shown in Fig. 2.6. The off-axis source point farthest from the optical axis in IMPOL, is about 15 mm away from the axis. The maximum inclination of the rays incident on the camera lens is about 5°. These extreme conditions are simulated by laser source. Firstly, on-axis point rays were simulated by keeping the laser source on the optic axis. It was observed that the rays corresponding to various angles of incidence within 5° inclination, actually pass out through the other side of the lens, unvignetted. The above test is repeated for off-axis source points within 15 mm of the optical axis. In all the cases, it was observed that the lens allows the rays to pass through it, unvignetted.

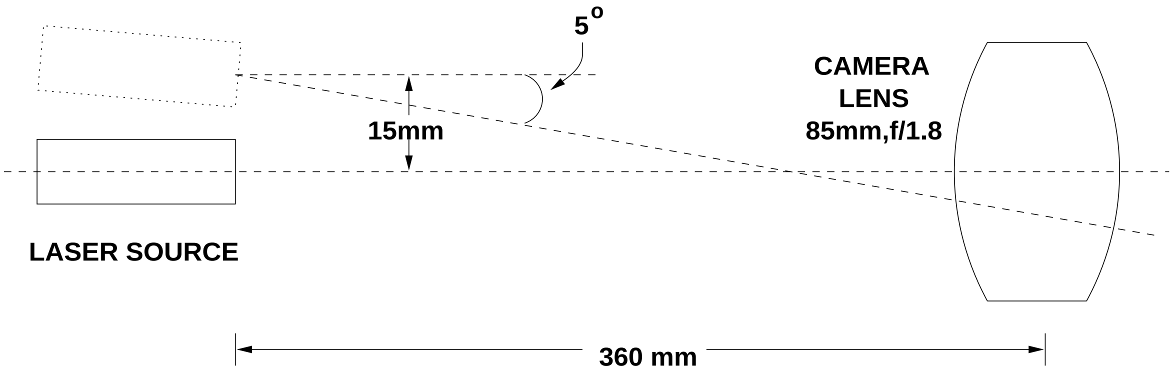

Figure 2.6: Schematic of the optical arrangement for testing the camera lens

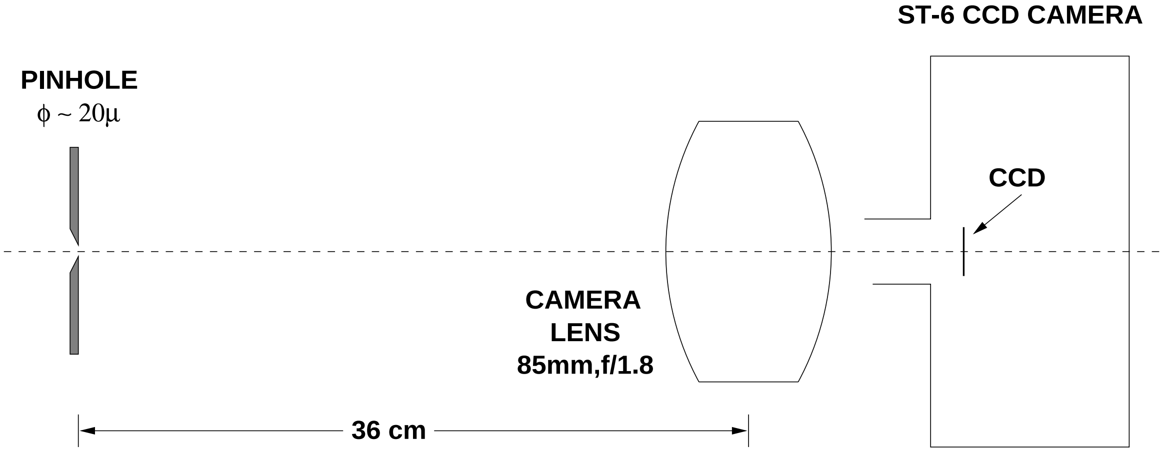

Figure 2.7: Schematic of the optical arrangement for determining spot size

Spot size

The second test which was conducted on the camera lens was to determine the spot size for various on-axis and off-axis source points. For this, a pinhole of 20 μm diameter is placed in front of the camera lens at a distance of 36 cm as shown in Fig. 2.7. The aperture of the lens is fully opened. For various values of the "focus" setting of the lens, the position of best focus is determined by moving the CCD camera along the optical axis. The pinhole is first placed on axis and the spot-size of the image on the CCD measured. The test is then repeated for positions within 15 mm of the optical axis and the degradation in the focus, if any, is noted. The FWHM, at best, was found to be about 65 μm for all these positions and this was obtained when the focus setting of the camera lens was at 0.85 m. The FWHM of the image could not be improved because, the copious infrared emission from the 3000K lamp source, which was used to illuminate the pinhole, was not filtered off, whereas the camera lens is not designed to perform well at these wavelengths.

2.3.4 Full assembly tests

As shown in Fig. 2.1, the grid of parallel obscuring strips is placed with its inner surface coinciding with the telescope focal plane. In this test assembly, a pinhole of 50 μm diameter is used at the position of the grid surface and the detector used is the ST-6 CCD camera from SBIG.

The field lens is placed about 20 mm in front of the telescope focal plane. It is an achromatic doublet of 50 mm diameter and 300 mm focal length. The half-wave plate (HWP) is placed at the focal plane of the field lens and has a clear aperture of 24 mm so as to avoid vignetting of the f/13 telescope beam. The maximum angle of incidence on the half-wave plate and the components following it, which this arrangement will produce, is less than 6°. Thus, by the time the beam reaches the camera lens, it will have a cross-sectional diameter of about 38 mm. The Wollaston prism has a clear aperture of 30 mm×30 mm and the filters have 40 mm diameter. The focal length of the camera lens is 85 mm and when its aperture is fully open it has a diameter close to 50 mm. The half-wave plate, the Wollaston prism and the filter assembly are placed as close together as is allowed by the demands of mechanical mounting.

The placement of the camera lens is determined by considerations of field of view and the image scale as well. Considering the VBT, which has a plate scale of about 7 arcsecs per mm at its Cassegrain focus, for a CCD chip of about 10×10 mm size, demanding a field of view of about 3.5 arcmin, will give an upper limit of 0.32 for the magnification in the system. On the other hand, on the same telescope, for a CCD chip of 20 μm pixels, demanding an image size of about three pixels under typical seeing conditions (2 arcsec), will give a lower limit of 0.21 for the magnification.

Table 2.1 contains a list of all optical components used for polarimetry in the instrument, their sources and some relevant information.

Determination of optical magnification

The magnification of the optical system was directly measured by the following method. The pinhole is mounted on a translational stage which can move it horizontally in the direction perpendicular to the optical axis of the system. The displacement of the pinhole can be measured with an accuracy of 50 μm. The optical system produce two vertically separated images of the pinhole on the CCD. The CCD is aligned so that the line joining the two images is parallel to the pixel columns. The pinhole position is noted on the vernier of the translation stage and an exposure is taken. The ADU counts in the pixels within a 5×5 array about each of the two images are noted. These are used to calculate the centroids of the images using the following formulae:

$$X_c = X_0 + \frac{\sum_{i=0}^{w-1}\sum_{j=0}^{h-1} \quad i \times [I(i,j) - B]}{\sum_{i=0}^{w-1}\sum_{j=0}^{h-1}[I(i,j) - B]}$$
$$Y_c = Y_0 + \frac{\sum_{i=0}^{w-1}\sum_{j=0}^{h-1} \quad j \times [I(i,j) - B]}{\sum_{i=0}^{w-1}\sum_{j=0}^{h-1}[I(i,j) - B]} \,, \tag{2.5}$$

Table 2.1: Optical components used in IMPOL

Component	Source	Part number	Description
Field lens	Karl Lambrecht	322305	50 mm dia., f=300 mm, AR coated, achromat
Half-wave plate	Karl Lambrecht	WPAC 2-22-BB400/700	achromatic, 22 mm dia. clear broad band single layer AR coated
Wollaston prism	Bernard Halle	PWQ 30.30	quartz, 29x29 mm clear multi layer AR coated
Filters	Andover		B, V and R, 40 mm dia., 5 mm thick, AR coated, image quality
Camera lens	Nikon		85 mm, f/1.8, AF

where (X_c, Y_c) are the centroid coordinates, (X_0, Y_0) are the coordinates of the pixel at the left-top corner of the array, (w, h) are the array width and height, $I(i, j)$ is the count in the pixel ($X_0 + i$, $Y_0 + j$) and B is the average counts in the background.

Now the pinhole source is moved by a known amount, another exposure is taken and the centroids calculated as before. Since the shift of images calculated from the difference in the image centroids is in pixels, we need to determine the horizontal pixel dimension to determine the magnification. For this, the CCD camera is mounted on a horizontal translation stage with a vernier scale and the pinhole is kept at the optical axis. Then exposures are taken after moving the CCD by known amounts and the image centroids positions are calculated. By taking the ratio of the motion given to the CCD to the corresponding difference in centroids, measured in pixels, the pixel dimension was determined to be 23 μm. Putting back this value into the earlier calculations, the magnification of the optical system was obtained as 0.26.

Determination of grid dimensions

The vertical dimension of the CCD pixels was calculated to be 27 μm through a procedure similar to above. From the readings of the experiment to determine the magnification, described above, the separation between the two images of the pinhole formed on the CCD was found to be about 705 μm. Now the width/separation required for the obscuring strips at the telescope focal plane is obtained as 705/0.26=2712 μm or 2.7 mm. However, to allow for tolerance in the dimensions while fabricating the grid of obscuring strips, while ensuring the separation of the ordinary and the extraordinary images, the strips are made 2.8 mm wide and are placed with gaps of 2.6 mm between them (see Fig 2.8).

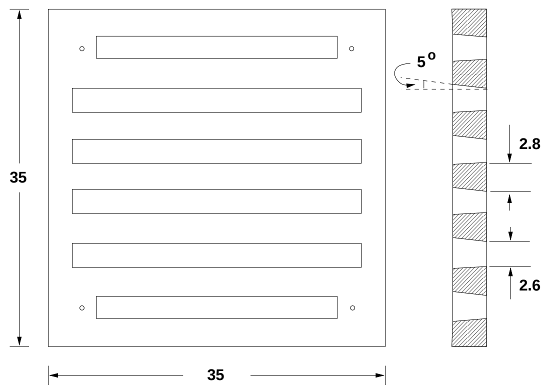

Figure 2.8: The grid of obscuring strips at the telescope focal plane

Miscellaneous tests and ghost images

After assembling the optical components as described above, and focusing the pinhole on the CCD, it was verified that a change in filter does not demand a shift in the image plane to keep the images well-focussed. It was also found that the rotation of the half-wave plate produces a shift of less than 0.4 pixels on the CCD.

Multiple reflections from the various optical surfaces result in ghost images of bright objects in the field. In the IMPOL optical system, three such ghosts are seen. The brightest of these is formed due to multiple reflections from the surfaces of the lenses in the camera lens. If the pinhole is moved in such a way that the main images move towards the right on the CCD, these ghost images are seen to move by about the same amount towards the left. The second pair of ghost images is produced by multiple reflections from the filter surfaces. These images are seen to move along with the main images and by about the same amount. The faintest pair of ghost images are the results of multiple reflections from the half-wave plate surfaces. These images are found very close to the main images and each rotates around its corresponding main image when the half-wave plate is rotated. The light in the ghost images is maximum for the R band and even in this case, the brightest ghost image is only $\frac{1}{2000}$ as bright as the corresponding main image.

2.4 Mechanical structure

All the optical components associated with polarimetry are enclosed in a cast aluminium pipe, which is about 200 mm in diameter and about half a metre long (see Fig. 2.9). This pipe is actually made of four separate sections, each acting as the support structure for the mounts of different optical components. These different sections are attached together with the help of flanges provided at their ends, which can be bolted together. Such an arrangement is useful, particularly while assembling and testing, since any part of the instrument can be accessed without having to dismantle the entire assembly. Additionally, these flanges are provided with mutually matching

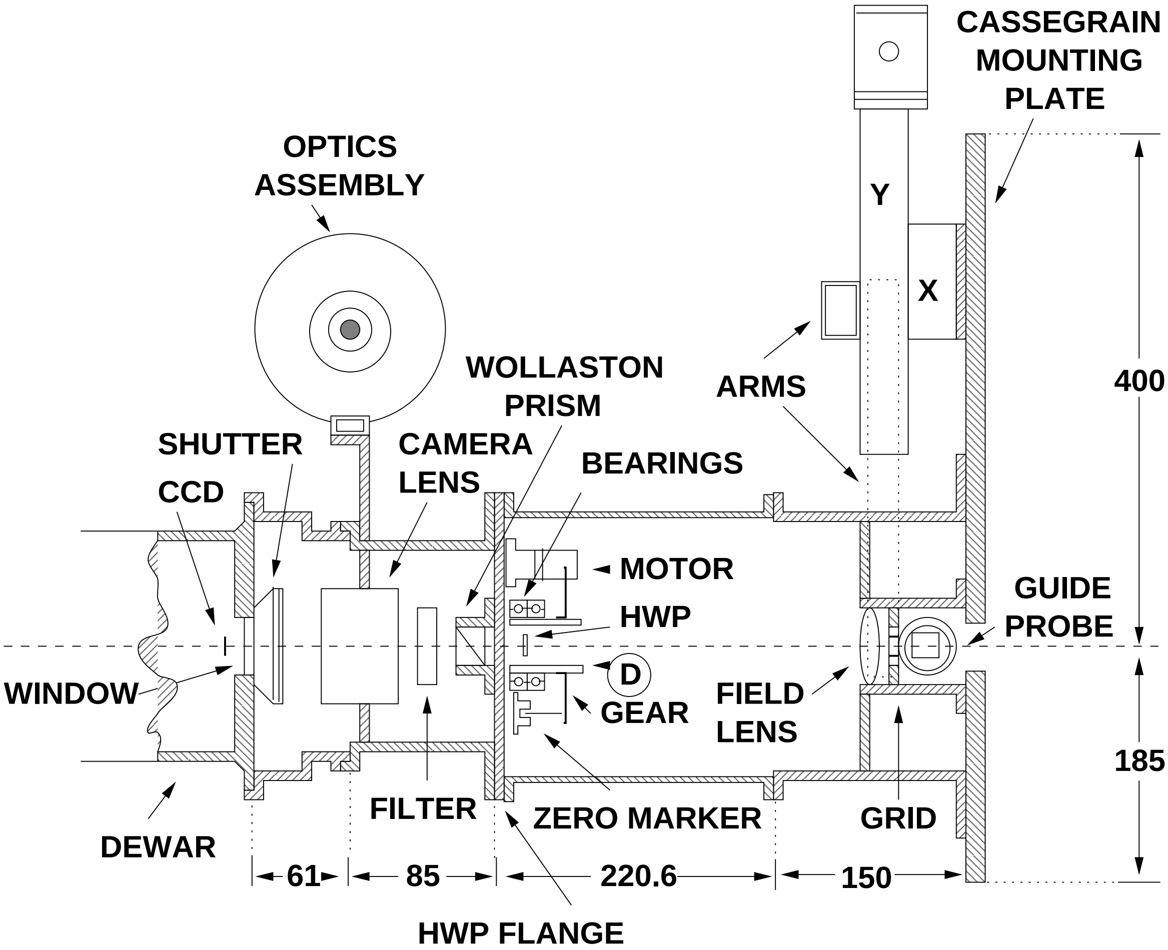

Figure 2.9: A block schematic of the IMPOL assembly mounted on the Cassegrain mounting plate.

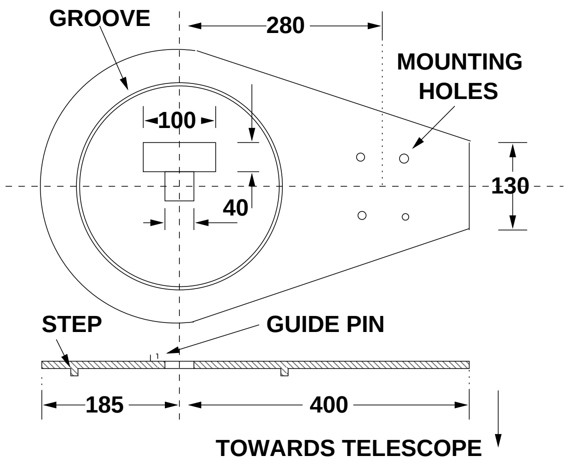

Figure 2.10: The Cassegrain mounting plate of IMPOL which ensures alignment of the optic axis of the telescope with that of the instrument. This plate also carries the XY translational stages of the acquisition and guidance system which is secured on the mounting holes shown.

grooves, steps and guiding pins, which are accurately machined, so that the central axes of the different pipe sections coincide to form a straight line, which defines the optic axis of the instrument.

The instrument is mounted on the telescope by means of a Cassegrain mounting plate which ensures that the optic axis of the telescope coincides with that of the instrument. This plate has a circular cross-section, but with a long extension towards one side (see Fig. 2.10), which carries the XY translational stages of the acquisition and guidance system (see Chap. 4). The instrument assembly is such that its optic axis passes through the centre of the circular part of the mounting plate. Right at the middle of the circular part of the plate, there is a 40×40 mm square hole which defines the field of view of the polarimeter. Adjacent to it, there is a rectangular hole 40×100 mm, as shown in Fig. 2.10, which defines the region of the sky from where a guide star may be chosen for the purpose of telescope pointing and guiding (see Chap. 4). The guide probe is attached to the XY translational stages and can be moved to any required position over the rectangular aperture (40×100 mm).

A schematic of the first section of the pipe is shown in Fig. 2.11. This 150 mm long section has 10 mm thick walls and has an inner diameter of 150 mm. The flange at one end of this section (the one with 300 mm diameter), is for bolting it to the instrument mounting plate, while the flange at the other end is for attaching to the second pipe section. An opening which is about 150 mm wide and about 38 mm high is provided on one side of the wall of the pipe, close to the 300 mm flange (see Fig. 4.2). This cutout is for the probe assembly of the acquisition and guidance system, to be positioned over the 40×100 mm opening on the Cassegrain mounting plate. Therefore, while mounting the pipe section on the Cassegrain mounting plate, it should be ensured that the wall opening is on the same side of the main field, as is the above opening of the Cassegrain mounting plate.

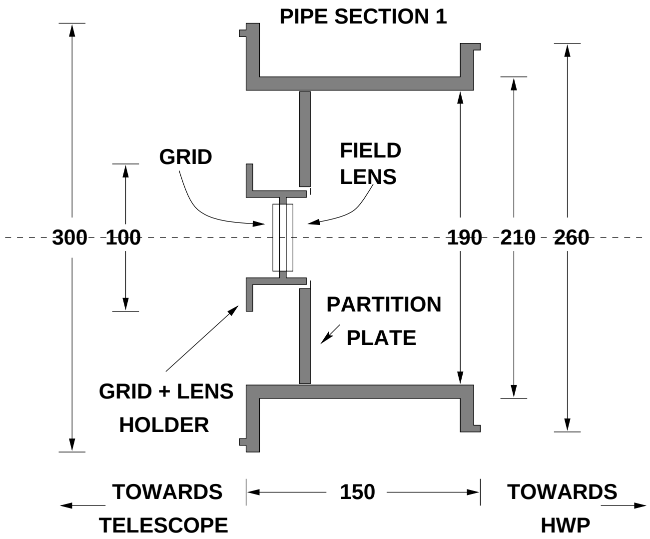

Figure 2.11: The first section of the pipe carrying the optical components.

The grid and the field lens are mounted on a single aluminium holder, which is fixed on the Cassegrain mounting plate, directly over the 40×40 mm opening. Pipe section number one is partitioned inside with a plate which has a central opening which loosely fits the top of the aluminium holder as shown in Fig. 2.11. This ensures that, once all the sections have been assembled, the chamber containing the half-wave plate, Wollaston prism etc. is isolated from dust, entering through the openings at the front.

Pipe section number two, is essentially a spacer, which covers most of the distance between the field lens and the half-wave plate. It is 216.7 mm long end to end and has inner and outer diameters of 200 mm and 210 mm respectively.

The most complicated assembly in the entire instrument is that of the half-wave plate (HWP) and the Wollaston prism, as illustrated in the block schematic of the assembly given in Fig. 2.9. The HWP, along with the gear mechanism for rotating it, as well as the Wollaston prism are attached on a single plate, marked as the *HWP flange*, in the drawing. This plate is held in position between the flanges of pipe section number two (the spacer pipe, which was mentioned above) and pipe section number three. A stainless steel cylinder (marked **D**) of 34.00 mm inner diameter, held on the inner races of two bearings, butted against each other, forms the rotatable housing which carries the HWP holder. The outer races of the bearings are pressed together and against a circular step in the middle of the HWP flange, by a lock ring arrangement. The stainless steel pipe also carries, on its outer diameter, a toothed brass gear with a PCD of 120.0 mm. This gear couples with another one with a PCD of 12.0 mm which is mounted on the shaft of a stepper motor, thereby giving a gear ratio of 1:10. The stepper motor itself is clamped to a surface of the HWP flange, using a bracket arrangement.

The Wollaston prism has a square cross-section, 30×30 mm in size, and has to be inserted in the beam path in such a way that the plane containing the ordinary and the extraordinary beams, is perpendicular to the orientation of the grid bars. These two directions fix the two reference axes of the instrument, orthogonal to the optic axis. The mount of the Wollaston prism has a circular perimeter and can be inserted into its holder in any orientation. The holder, in turn, is bolted to the HWP flange. Once the Wollaston prism mount is rotated to the correct orientation, it can be fixed to the holder using grub screws.

The HWP is a very delicate component, about 25 mm in diameter and about 0.8 mm thick. While designing a mount for the HWP, care is taken to ensure that the difference in thermal expansion rates of the mount material and the component, does not lead to stress birefringence effects. The same is true in the case of the field lens and the Wollaston prism. The key idea behind the design of the mounts, is to keep the points of attachment between the component and its mount in a plane and to ensure that all the points of the mount except one, have enough flexibility along the plane, to adjust for differential thermal expansion, thereby minimizing stress on the components themselves. Since the HWP acts also as the aperture stop of the optics, an annular black mask is placed over it, to ensure that light does not get scattered from the mount or the edge of the HWP itself (see Fig. 5.5).

The third section of the pipe carries the filter rails and the holder for the camera lens. The filter rails allow a long holder carrying different filters to be slid into the beam path. Provision is also made to fix the position of the holder on the rails, when any one of the filters is in the beam path. Each holder (there are two) can carry three filters, each of about 40 mm diameter and about 5 mm thick. The filter complement of IMPOL includes Johnson B, V, R filters and a wideband filter made of Schott KG3 glass, which has a passband that roughly corresponds to the combined B, V and R bands and cuts off I band. The filter holder is moved in/out on the rails, manually.

The camera lens is mounted on a plate which has a locking arrangement at its centre, similar to the one usually provided on the chassis of cameras with detachable lenses. This plate is bolted on to a holder which in turn is fixed on a groove, that is provided on pipe number three, for the purpose.

The last section of the pipe serves two purposes. The liquid nitrogen dewar which carries the CCD chip is fixed on a flange of this pipe and it acts as a spacer which ensures that the CCD surface comes at the correct distance behind the camera lens. Secondly, the coupling arrangement of this section with the one before (the third one) is such that it allows the CCD dewar to be rotated about the optic axis and fixed at any orientation. This is useful to ensure that the rows/columns of the CCD are aligned with respect to the axes of the instrument, as defined by the orientation of the grid and the fast axis of the Wollaston prism. A shutter, which allows to control the timing of exposures and to take dark frames, is mounted on the flange of the dewar.

2.5 Electronics

The electronics associated with the instrument can be broadly classified under two heads – instrument control and data-acquisition. These two aspects are fully isolated in the case of IMPOL, each having its own computer and separate communication links to the instrument. This isolation came about since the CCD-based data-acquisition system was developed as a separate project at IUCAA, to be a general purpose facility, the first application of which is the imaging polarimeter. In the next section we discuss the various aspects of the instrument control electronics, while only the relevant details of the data-acquisition system is briefly dealt with, in the section following it (see Deshpande & Gadre 1994 for more details).

2.5.1 Instrument control

There are two subsets of operations involved in instrument control – (i) the positioning of half-wave plate at the correct orientation and (ii) the sequencing and execution of the steps involved in moving the guide probe to acquire the guide star and do auto-guiding. A large part of the electronics is common to these two, or at least consists of similar subunits. The following discussion will concentrate on these common features as well as the details directly related to the positioning of the HWP. Since Chap. 4 is dedicated exclusively for the discussion of the acquisition and guidance system, all the details of direct relevance to that are discussed there.

Almost all the electronics necessary for instrument control is enclosed in a box, about $300 \times 150 \times 100$ mm in size, which we will refer to as the *IMPOL control box.* There are two circuit cards in this box; the first is an embedded microcontroller card built around the Intel 8052-BASIC IC (the controller card) and the second one (the interface card) generates drive signals for activating the stepper motors and provides feedback to the controller card. A block schematic representation of the two cards and the interconnections between them are shown in Fig. 2.12. Explanations of the various blocks and their working are given in the following subsections. A substantial part of the work associated with the development, assembling and testing of the instrument control electronics and the assembler programs residing in the 8052 controller was carried out as a project by P. A. Chordia and R. Bedade as part of the requirements for their B. E. degree.

The controller card

The 8052-BASIC microcontroller is a versatile IC, particularly suited for embedded applications. It has an on-chip ROM with an in-built interpreter for a set of BASIC-like commands. On powering up the IC, this interpreter is run and the microcontroller just waits in anticipation of a command transmitted over its asynchronous serial communication port. Once a command is received, it is interpreted and an appropriate action taken. These actions mostly involve simple tasks like changing the state of a pin of an

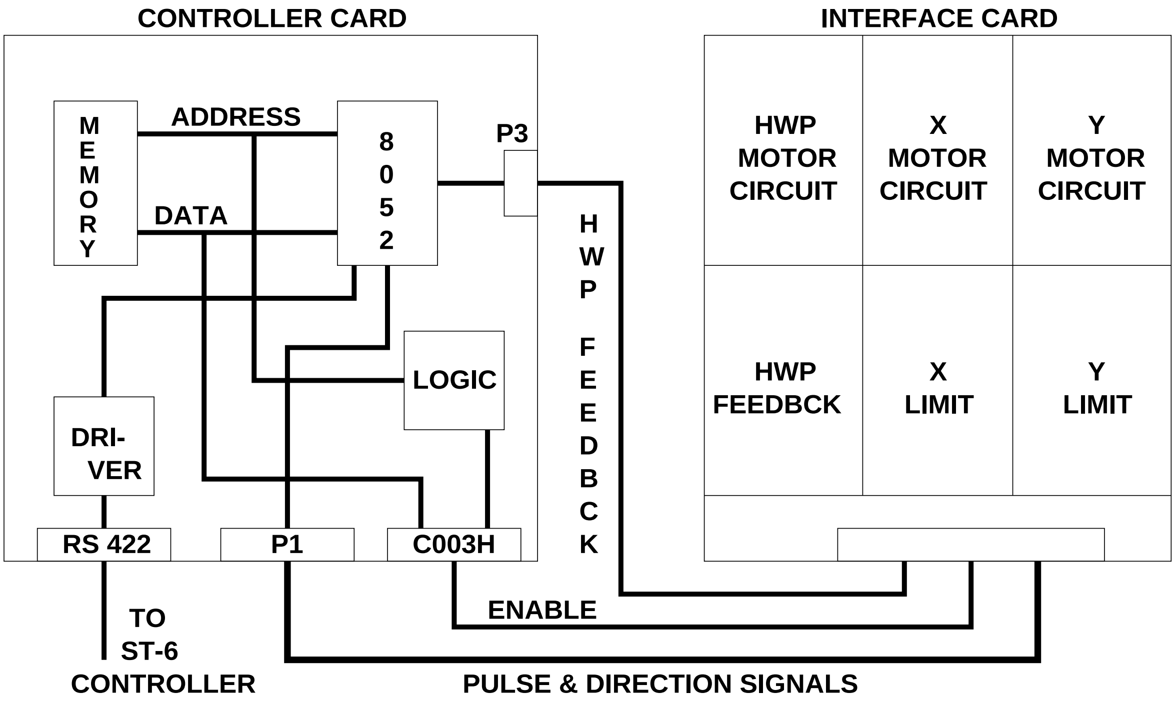

Figure 2.12: A block schematic representation of the two cards in the IMPOL control box and the interconnections between them.

output port, reading in the state of a pin of an input port etc. This is the "command" mode of operation. However, there is also another mode of operation called the "program" mode. In the program mode, instead of executing one command at a time, a sequence of commands may be given, as a program, at the end of which an instruction may be given to interpret and execute these commands sequentially, beginning from the first one. The microcontroller has also a complete set of assembler instructions each of which corresponds to a primitive task like moving the contents of a register, adding to the accumulator, reading from or writing to a memory location etc. A code made of these instructions can be stored in a sequence of memory locations and executed one after the other with a single "CALL first_memory_location" command. At the end of executing the assembler code, the control returns to the BASIC interpreter.

The 8052 IC has an 8-bit data bus and a 16-bit address bus. Out of the 64 Kb address space available, 32 Kb has been linearly mapped to a RAM (MC 62256), of which the first 16 Kb (address 0000H to 3FFFH) are used by the IC for its interpreter etc., while the other 16 Kb (address 4000H to FFFFH) is available externally for storing code or data. In addition to this, the board also provides four memory-mapped ports with addresses from C000H to C003H, some of which are used for generating control signals, as described in Sec. 4.3.2.

The controller card communicates with the control computer, using the asynchronous serial communication port mentioned above. The signal ground of the card is isolated from that of the communication link by means of opto-isolators (6N137) provided on the card. Differential driver buffers (MC 3486 and MC 3487) are used to make the link conformable with the RS 422 standard.

Translators and Drivers for the stepper motors

The three positioning requirements of the instrument, namely, the HWP rotation and the motion along two perpendicular directions, of the acquisition and guidance system probe, are achieved using three stepper motors, one for each motion. Each stepper motor has four windings or phases, which have to be activated in a certain sequence by passing current pulses through them, in order to make the shaft rotate. with the 1:10 ratio in the gear mechanism (see Sec. 2.4 which couples the shaft to the HWP mount, one rotation of the HWP takes 2000 steps, thereby giving a angular positioning resolution of $0.18°$. The nominal positioning error at any step position of the stepper motor is 5% of the mean step size.

There are three identical circuits in the interface card, each consisting of a translator and driver for a stepper motor. The translator receives digital control signals from the microcontroller, based on which, it generates the four phase signals in the proper sequence. These signals are then given to the driver, which amplifies them to the power required to excite the motor windings and make the shaft rotate. Three control signals are sent by the microcontroller to the translator – the "enable/disable" signal which connects/disconnects power to the motor windings, the "pulse" signal which decides the number of steps through which the shaft rotates (equal to the number of pulses in the signal) and the "direction" signal which controls the direction in which the shaft rotates.

Two ICs – L297 which is the translator and L298 which is the driver, are used to drive the motor windings. Figure 2.13 is a circuit diagram which shows the various interconnections between the ICs and the connections to the windings of a motor. The stepper motor which rotates the HWP, takes an average current of 0.4 A per winding with a supply voltage of about 12 V and provides a torque of about 8 Ncm at the shaft. The electric current which flows through the windings W1 and W2 (W3 and W4) also flows through the sense resistor R1 (R2). When the voltage across this resistor crosses above a threshold value, the supply to the windings are disconnected and it is reconnected as soon as the voltage falls below the threshold. This chopping (turning off and on) occurs at a much higher frequency compared to the fastest "pulse" signal rate and is useful as a means of controlling the average current that flows through a winding when it is activated.

Half-wave plate position control

Pins numbered 0 and 1 of the IO-mapped port, P1, of the IC are used to generate the pulse and direction signals for moving the HWP and the seventh pin of the memory-mapped port at C003H provides the enable/disable signal. The discussion in Sec. 2.2 clearly illustrates that observations at at least two specific orientations of the HWP are necessary to recover fully the linear polarization information in light. In order

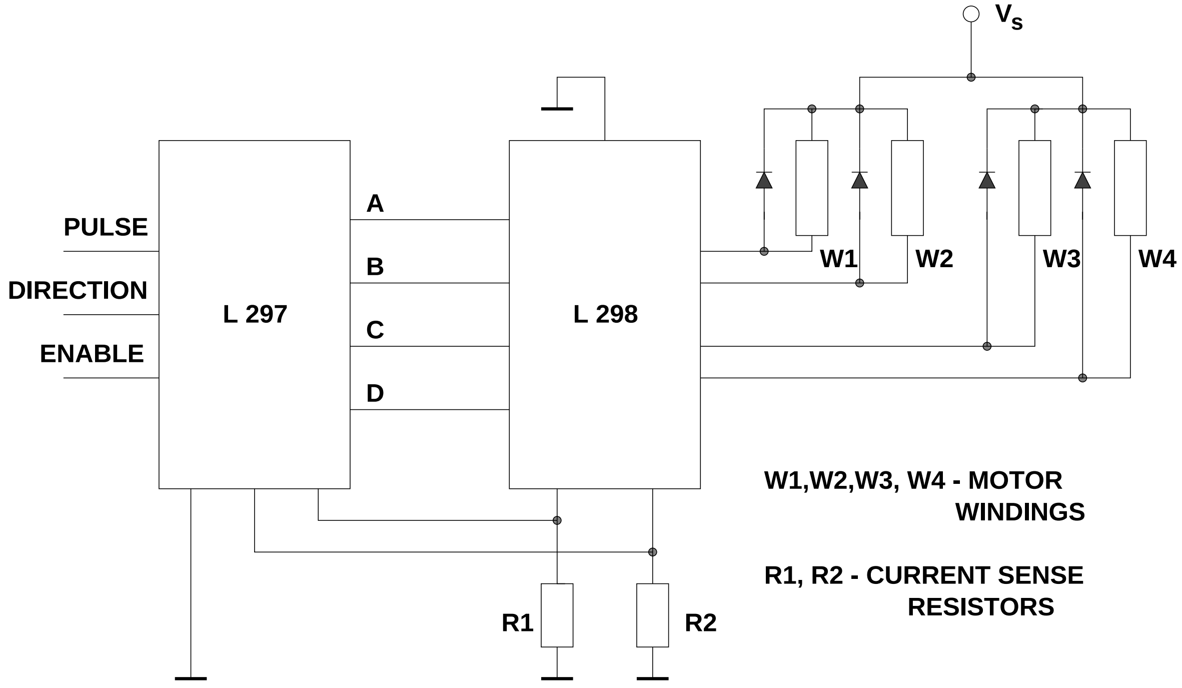

Figure 2.13: The circuit generating the drive pulses for exciting the stepper motor windings.

to ensure that the HWP can be positioned accurately and repeatably at the correct orientations, a zero marker is provided. This consists of a unit carrying an infrared light emitting diode (LED) and a phototransistor mounted on the HWP flange. Normally, light from the LED falls on the phototransistor, except when the HWP is close to its zero position, causing an interrupter attached to the larger gear wheel, to block the light. This change in light level on the phototransistor is detected using an electronic circuit, as shown in Fig. 2.14 and fed to the third pin of the IO-mapped port, P3, of the IC. Whenever it is required to move the HWP to zero position, the microcontroller checks for a change in the signal level at this pin, after generating every pulse. Once it detects such a change, it stops the rotation and moves the HWP back, once step in a second, till it finds that the feedback signal changes back again. This ensures that the HWP is positioned exactly at the position where the interrupter just moves out of the beam path. Two more precautions are taken to ensure the repeatability of zero positioning. The opening through which light falls on the phototransistor is made very narrow - about 50 μm and secondly, the HWP is rotated in the same direction while seeking the zero position. Once the zero position is detected, rotating through 125 steps moves the HWP to positions 22.5°away, as required.

2.5.2 Image acquisition

As mentioned previously, the CCD camera system was developed as a separate project in IUCAA and only those aspects of the system which is of direct relevance to this

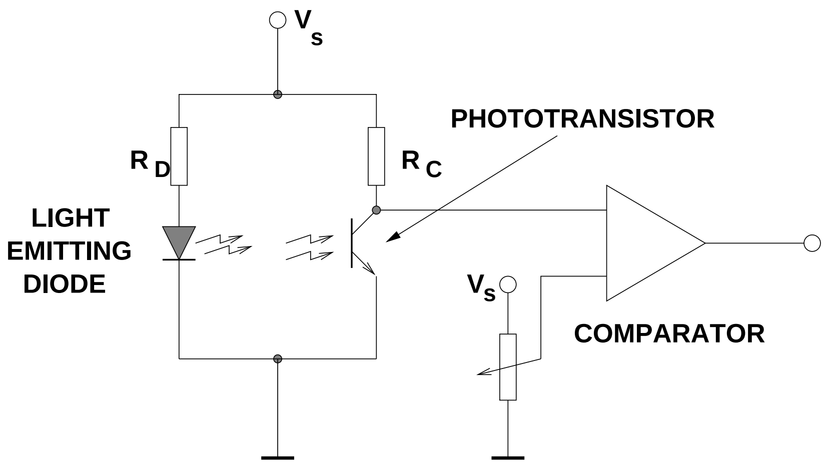

Figure 2.14: The zero marker circuit to ensure accurate and repeatable zero positioning of HWP.

thesis work are mentioned here. More details of this system are available in Deshpande & Gadre 1996. The data-acquisition system is built around an EEV CCD chip, which has an array of $385 \times 578, 22\ \mu m$ pixels. The CCD is mounted in a dewar, which can be filled with liquid nitrogen during observations for cooling the CCD. Apart from the dewar, the data-acquisition system consists of three other sub-assemblies, namely the embedded controller, the CCD controller and the host computer (PC 486), as shown in the block schematic of Fig. 2.15.

The embedded controller is based on Intel 8052-BASIC and is very similar to the one which was described earlier in Sec. 2.5.1. According to the commands received from the host computer, the embedded controller selects the correct format of the control signals, times exposures by opening and closing the shutter as well as monitors and controls the data retrieval and transfer to the host computer. The host computer communicates with the embedded controller over an RS 422 link. There is also a feedback control mechanism which maintains the temperature of the CCD at the user-defined preset level. The CCD controller generates the clocks, bias voltages and other signals for retrieving the analogue signal from the CCD; amplifies, samples and integrates this signal and finally convert it to digital form. The digitized output from the CCD controller is transmitted to the computer through a high speed (1Mbaud) dedicated link, and is converted to parallel data and accumulated in the memory.

Some parameters relevant to the data-acquisition system and its performance are listed in Tab. 2.2.

2.6 Software

As in the case of electronics discussed above, here also, the two aspects – instrument control and data-acquisition – are totally isolated and are discussed separately in the following two subsections. The data-acquisition software was primarily developed by

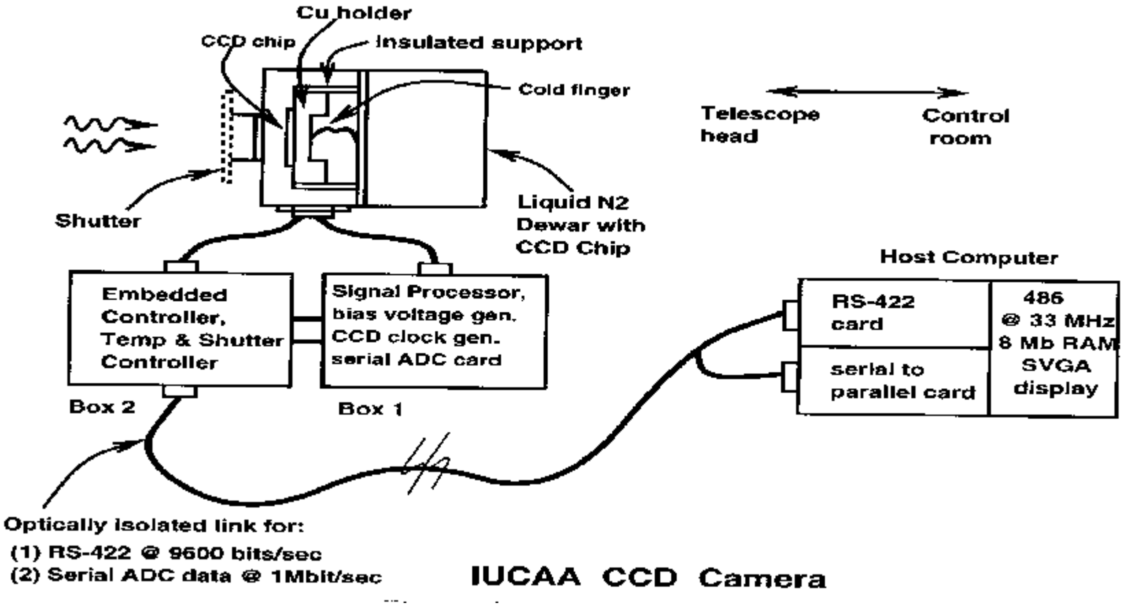

Figure 2.15: Block schematic representation showing the various subassemblies of the data-acquisition system (adapted from Deshpande & Gadre 1996).

Table 2.2: The parameters of IUCAA CCD Camera

Parameters	Value
CCD make	EEV CCD02-06 series
CCD chip size	385(H)$\times$578(V)
Pixel size	22×22 μm
Active area	12.7 mm $\times$ 8.5 mm
No. of amplifiers	1
Quantum efficiency	blue : 20%
	yellow : 50%
	red : 60%
Host	PC 486
Readout speed	32 μs per pixel
Acquisition & Display time	12 s (full frame)
Read noise (total)	8 e^- rms
Gain	5 e^- / ADU

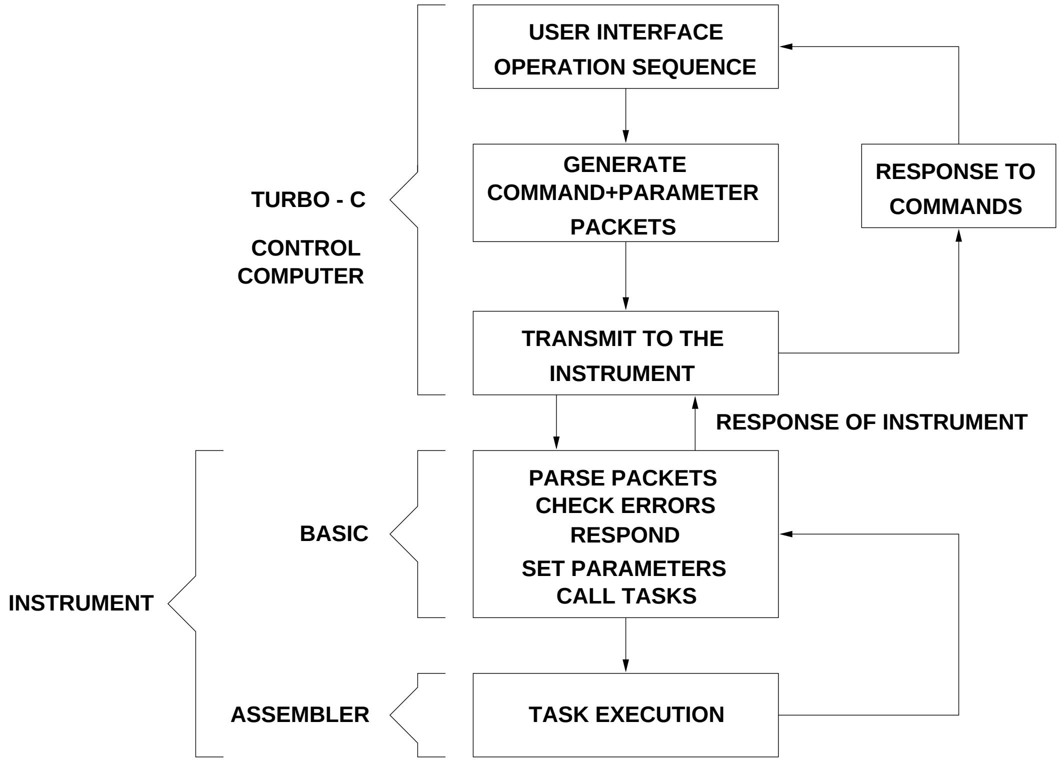

Figure 2.16: The structure of the instrument control software.

D. V. Gadre and adapted for IMPOL by T. Deoskar as part of the latter's B. E. project.

2.6.1 Instrument control

The instrument control software is structured in five layers as shown in Fig. 2.16. The uppermost three layers are written in Turbo-C and reside in the control computer, the fourth and fifth layers are in BASIC and 8052-assembler, respectively, both reside in the memory of the microcontroller for instrument control, described in Sec. 2.5.1. All instrument control operations are initiated at the topmost layer, either during initialization at the time of start-up or during observations. The operations carried out at the time of initialization, depends on the contents of the configuration files which are read following start-up. During observations, most of the actions are taken at the instance of the user.

Except in cases where the required operation is local to the control computer (for example, a change of mode, of the software from HWP control to acquisition and guidance control), the topmost layer generates a service call to the second layer. This layer creates a "command+parameter" packet depending on the service requested and the current system configuration. For example, if it is required to change the HWP position, the packet will contain the appropriate command followed by the number of steps, direction and the speed with which to move the HWP. This packet is then passed on to the third software layer, which sends it to the controllers at the instrument, over the asynchronous serial communication link. Upon receiving such a "command+parameter" packet, the controller at the instrument, parses it and checks for errors. If the command is valid and there are no errors, it immediately sends back an acknowledgement signal. Otherwise, it sends back a corresponding error signal. The result of this communication process is conveyed back to the topmost layer for appropriate follow up. The fourth software layer is a BASIC program which resides in the memory of the 8052-based microcontroller and carries out the processes of packet reception, parsing, error checking and acknowledging. A set of assembler routines, each doing a specific operation, forms the fifth and lowermost software layer. The BASIC program stores the parameters at specified memory locations and calls one of these assembler routines to execute the particular task, requested by the command.

Many of the tasks, such as the positioning of the HWP, takes a finite amount of time to complete, during which period, the microcontroller will not accept another command. But the control computer can send a query to find if the execution of the previous task has been completed. Then, the microcontroller will send an "execution-completed" signal, when it is ready to receive another command.

Initialization

After powering up the system, once the software is started, it first reads a configuration file, called IMPOL.CFG, which contains information such as the communication port of the computer to which the instrument has been connected, the baud rate which is to be set up for communication, the names and locations of the files containing the BASIC and assembler programs which are to be downloaded to the IMPOL controller etc. The software then establishes communication with the instrument at the required baud rate, failing which, it indicates so, with an error code corresponding to the type of failure. Upon success, it transmits a BASIC program, called INIT.BAS, to the IMPOL controller, and runs it (see Sec. 2.5.1), the purpose of which is to set the signals at all the ports of the controller to their default levels. This is followed by the transmission of another BASIC program called ACCEPT.BAS. This program is designed to accept a series of assembler routines and store them in specific locations in the memory of the 8052 controller card (D. Gadre 1995). These are the assembler routines which when called execute specific tasks like connect/disconnect the power to the stepper motors, zero position the HWP, move it by a specified number of steps in the specified direction etc. Once these routines are stored in the correct locations, one more BASIC program called COMMAND.BAS is transmitted and run. It is this program which receives instrument control "command+parameter" packets from the computer and does the parsing, error-checking etc., as has been explained above. The last step in the initialization procedure is to send commands to the IMPOL controller to zero position the HWP and the probe assembly of the acquisition and guidance system.

It is to be noted that, it is necessary to go through the above steps of initialization only once after powering up the system. After that even if one exits the software and restarts it, there is no need to repeat all the steps, because, the necessary BASIC and

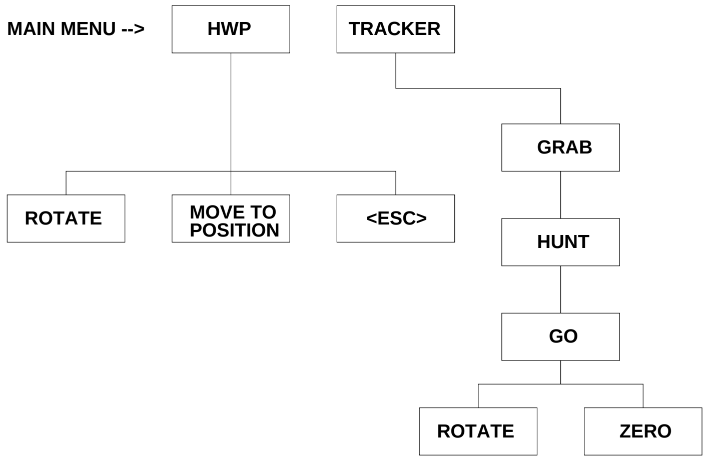

Figure 2.17: The menu structure which allows various operations related to HWP position control.

assembler programs are still available in the memory of the IMPOL controller. In fact, once the software is started, it actually queries the user before beginning to transmit the files as also before zero positioning the HWP and the probe.

Half-wave plate position control

Here, we briefly look at the various options provided by the software to position the HWP, while the corresponding discussion relevant to the acquisition and guidance system has been deferred till Chap. 4.

The menu structure of the software related to the HWP control mode is shown in Fig. 2.17. The software is switched to HWP control mode by selecting the option *HWP* in the main menu. The process of selecting any menu item is just pressing the corresponding highlighted letter on the keyboard. There are two ways of moving the HWP. The first (*ROTATE*) is to move the HWP by a fixed number of steps, in either direction at a specified speed of rotation. The second (*MOVE TO POSITION*) is to position the HWP at any of the four orientations, namely, 0°, 22.5°, 45°or 67.5°. Once this option is chosen, the HWP is first moved to the zero position where the feedback is available and then by the appropriate number of steps, to bring it to the required orientation. There is also a provision to position the HWP, while the auto-guiding is going on. This is possible while the software is in the *TRACKER* mode, as shown in Fig. 2.17. *ROTATE*, here, has the same meaning as under the *HWP* option, while *ZERO* allows the HWP to be moved to zero position.

2.6.2 Image acquisition

The software for data-acquisition consists of two programs, both written in Turbo-C. The first of these, is an editor, which allows the user to create and save a disk file, that contains the values of various parameters relevant to an exposure. Examples are exposure time (which can be set in multiples of 55 ms), type of exposure – dark/light, that is whether the shutter should be opened or not during the exposure etc.

The second program, when run, initializes the computer memory by emulating the 8 Mb RAM of extended memory available as expanded memory and then asks for the name of the file from which the exposure parameters are to be read. Then it commands the CCD controller to take an exposure and acquires the digitized data into its memory. This image is displayed on the monitor and the user can inspect the data by moving a cursor around, and checking the pixel value displayed at each position. There is also a provision for adjusting the contrast of the display by changing the minimum and maximum pixel values which should correspond to the minimum and maximum grey levels that can be displayed on the screen (see App. E for more details).

The user can then decide whether or not to save the file on the disk, and then whether to continue with taking another exposure with the same/another parameter file. The images are saved in ASCII format and hence occupies about 1.2 Mb per full frame. A third Turbo-C program is used to read these files and convert them to FITS format. The FITS header in these files contain the values of all the parameters which are set in the parameter file.